Nanoscale Systems for Optical Quantum Technologies

Grant Agreement No: 712721
Start Date: 1st October 2016 - Duration: 36 months

D2.2 Ensemble coupled to cavity

Deliverable:	D2.2
Work package:	WP2 Spin atom photon interfaces
Task:	2.1 Purcell-enhanced readout of a single Eu3+ ion
Lead beneficiary:	KIT
Type:	Report
Dissemination level:	Public
Due date:	30 September 2017
Actual submission date:	25 September 2017
Author(s):	David Hunger (KIT)

This project has received funding from the European Union's Horizon 2020 research and innovation programme under grant agreement No 712721.

Version history

Version	Date	Author(s)	Description
V1	1/09/2017	D. Hunger (KIT)	First draft
V2	12/09/2017	D. Hunger (KIT)	Revised version, inputs from P. Goldner, H. de Riedmatten, B. Casabone

Table of Contents

Deliverable Description

This deliverable reports work at KIT to demonstrate first coupling experiments of Eu ion ensembles to a fibercavity under cryogenic conditions. This represents an important intermediate step in the course of the project that validates the functionality of the built laser system, the optical microcavities, the cryogenic nanopositioning stage, and the detection approach. We have successfully detected cavity-enhanced fluorescence from an individual nanocrystal, and from an evaluation of the detected signal, we can infer an estimate of the achieved Purcell enhancement.

Experimental setup

For the experiments, we use the cryogenic cavity setup based on a commercial attocube nanopositioning stage (see D.1.1). This setup provides full functionality to spatially scan the sample along 3 axes with about 2µm closed loop resolution. We use this to implement scanning cavity microscopy to locate suitable nanocrystals inside the cavity, and to set the mirror separation to a particular longitudinal mode order to achieve resonance conditions with the ions.
We have also set up a frequency doubled grating stabilized diode laser providing up to 10mW of 580nm light with a short term linewidth of about 30kHz. The laser is tunable via its external grating and the diode current, and the optical setup contains an AOM for pulsed excitation and for multi-frequency spectroscopy. We are currently preparing an external reference cavity (high vacuum, triple temperature shield, temperature stabilization) to stabilize the laser frequency to a sub-kHz level.
For detection, we use an APD with a high quantum efficiency at 580nm (~70%) and low dark counts (~20 counts/s).

Sample characterization

Before placing the sample in the cavity, we study the properties of the nanocrystals with a confocal setup to obtain reference values of optical properties and to optimize the preparation. The particles of 0.5% Eu^{3+}:Y_2O_3 were synthesized by CNRS-CP. Figure 1a) shows a confocal fluorescence image of individual nanocrystals (average diameter ~300nm, containing about 10^6 ions per crystal) spin-coated on a mirror. Analogous measurements were also performed with smaller nanocrystals, also prepared by CNRS-CP (average diameter 100nm), which were then used for the cavity experiments.

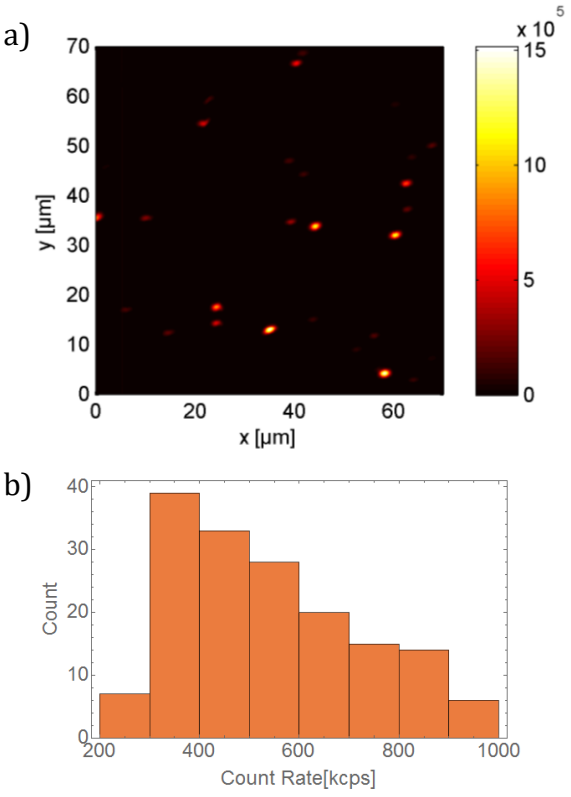

Fig. 1: a) Confocal fluorescence image of Eu:Y_2O_3 nanocrystals on a cavity mirror. b) Histogram of the count rate per nanocrystal as observed for a large number of individual nanocrystals.

Brightness distribution and single ion count rate estimate

We study a large area of the mirror containing a large number of isolated nanocrystals and infer the peak count rate per crystal. By looking at the count rate distribution and comparing with a size distribution as obtained from SEM imaging, we can get an estimate for the typical count rate per single ion, (see Fig. 1b). We excite under saturation conditions (~1mW, NA=0.95) with 532nm light and observe count rates of 10^5 to 10^6 photons/s. This shows that even with a high NA objective and with nanocrystals placed on a mirror, we only detect about one photon per second per ion in free space in saturation. This count rate can serve as a reference for comparison with the cavity-enhanced count rate (see below).

Single nanocrystal spectra

We furthermore record spectra of individual crystals and assess the room-temperature linewidth of the $^5D_0$-$^7F_0$ transition, which gives a first impression of the crystal quality. Figure 2a) shows a broadband fluorescence spectrum of a single crystal, the inset shows the $^5D_0$ - $^7F_0$ transition in high resolution. We observe a linewidth of 0.1nm (80GHz) for many crystals, which is as narrow as in good bulk samples, see Fig. 2b. Importantly, the same linewidth is also found for small nanocrystals with very low count rate which are compatible with cavity experiments.

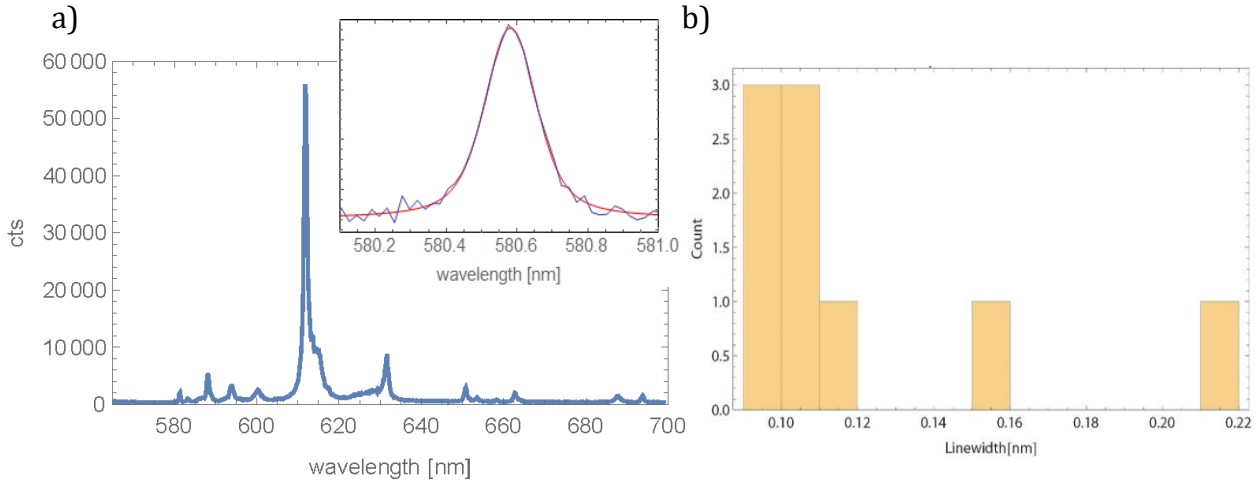

Fig. 2: a) Fluorescence spectrum of an isolated Eu:Y_2O_3 nanocrystal on a cavity mirror excited with 1mW 532nm light. The inset shows a high resolution measurement of the $^5D_0 \rightarrow {}^7F_0$ transition. b) Histogram of the observed fluorescence linewidth.

Fluorescence lifetime

Finally, we study the fluorescence lifetime, which is important as a reference when comparing with cavity measurements in the future, and which also gives some insight into the crystal size and the local environment of the nanocrystal. In particular, we observe a direct correlation between the lifetime and the count rate, see Fig. 3. This is related to the fact that a nanocrystal has a reduced local density of states (LDOS) for electromagnetic modes, due to the boundary condition of the crystal-air interface which makes the crystal

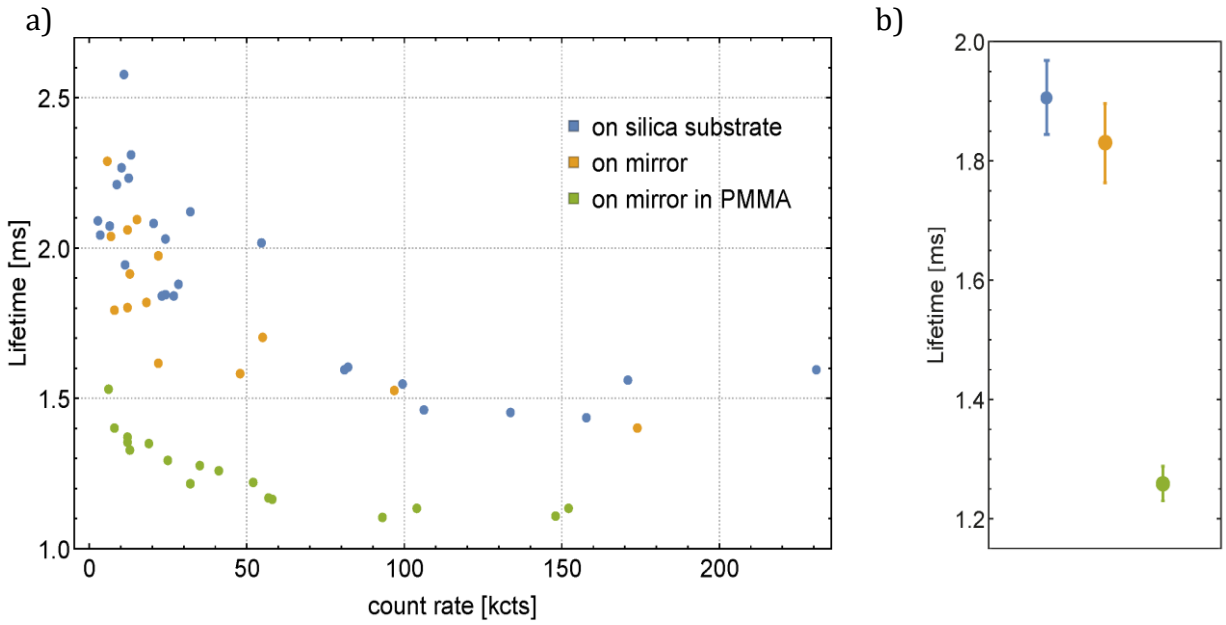

Fig. 3: a) Fluorescence lifetime measured for several nanocrystals and plotted as a function of the count rate, which is indicative of the crystal size. Measurements for crystals placed on a silica substrate, on a cavity mirror, and on a cavity mirror embedded in a PMMA layer are shown. b) Average lifetime observed for the three cases. Color code as in the left panel.

act as an off-resonant cavity (H. Schniepp). Smaller crystals have a smaller LDOS and thus a larger fluorescence lifetime. This trend is clearly visible in Fig. 3a). The difference of the emission lifetime for crystals placed either on a silica substrate or a mirror appears to be small. The mirror with a proper spacer should lead to constructive self-interference of fluorescence and thereby reduce the emission lifetime by about a factor 1.3. In the measurement this is not visible, since at the same time, the presence of the mirror and the reduced lifetime increases the fluorescence yield and thus shifts the datapoints for a given crystal size to the right, masking the effect. To fully evidence this effect, a measurement of the crystal size would be required. Finally, we can also observe the effect of embedding the crystal in a dielectric medium, which increases the LDOS, and leads to a marked reduction of the lifetime in the measurement. Figure 3 b) shows the lifetime for the three cases when averaging over all crystals.

Selection of suitable crystals

We use the scattering loss signal of nanocrystals to spatially locate a well isolated crystal of suitable size within the cavity mode. Therefore, we use scanning cavity microscopy (M. Mader), which we have implemented for the attocube stage in the cryostat. We evaluate the cavity transmission at 580nm to infer the scattering loss, and from this deduce the crystal size (see D1.1). We select crystals that are large enough to provide a suitable ion ensemble for first measurements, but small enough to maintain the outcoupling efficiency of the fluorescence light from the cavity at a high level. Figure 4a) shows a schematic drawing of the setup including the laser-machined fiber and the planar mirror carrying the nanocrystals. Figure b) shows a scanning electron microscope image of a Eu:Y_2O_3 nanocrystal, and Fig. 4b) shows the scattering loss of a single crystal when scanning the cavity mode across it. From the peak loss observed for perfect spatial alignment, we can calculate the crystal size, which amounts to 80nm for this measurement. Together with the doping concentration, this allows us to estimate the number of ions contained in the crystal, and we obtain a value of 10^4 ions.

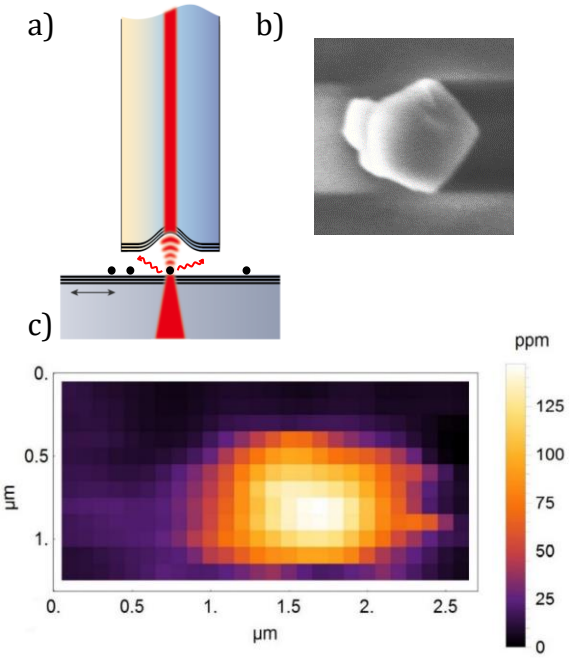

Fig. 4: a) Schematic drawing of the setup. b) Scanning electron microscope image of a single Eu:Y_2O_3 nanocrystal with 150nm diameter. c) Scanning cavity microscopy of the scattering loss of an isolated nanocrystal in the cavity.

Cavity-enhanced single nanocrystal spectroscopy

We studied the crystal that was characterized above with cavity-enhanced spectroscopy. The sample was cooled to a temperature of about 10K during these measurements.

Detection approaches

To obtain a fluorescence signals from the cavity, we consider two alternative approaches: We either excite the ions resonantly at 580nm and detect the subsequently emitted light at the same wavelength via temporal discrimination, or we excite at 580nm and couple the dominant emission of the $^5D_0$ - $^7F_2$ transition at 611nm to the cavity. While the former scheme will be important for later stages of the project, the large branching ratio into the $^5D_0$ - $^7F_2$ transition can be promising to increase the detectable count rate at least for a moderate finesse cavity. Since the final state decays via phonons, lifetime broadening increases the linewidth and might thus limit the Purcell factor for a narrow cavity linewidth. Also, the second scheme requires both the excitation light at 580nm and the emission light at 611nm to be resonant with the cavity. In addition, locking light at yet another wavelength needs to be resonant as well, making this scheme very restrictive and

difficult. Still, for the first attempt, we use this strategy due to the initially larger fluorescence yield.
Figure 5 shows the principle of the scheme. The right longitudinal cavity mode order needs to be selected to achieve resonance conditions for the two transitions. The resonance spectrum of the cavity for longitudinal mode orders q=17...21 are shown, and a calculation of the expected count rate as a function of q as well as a measurement are shown.

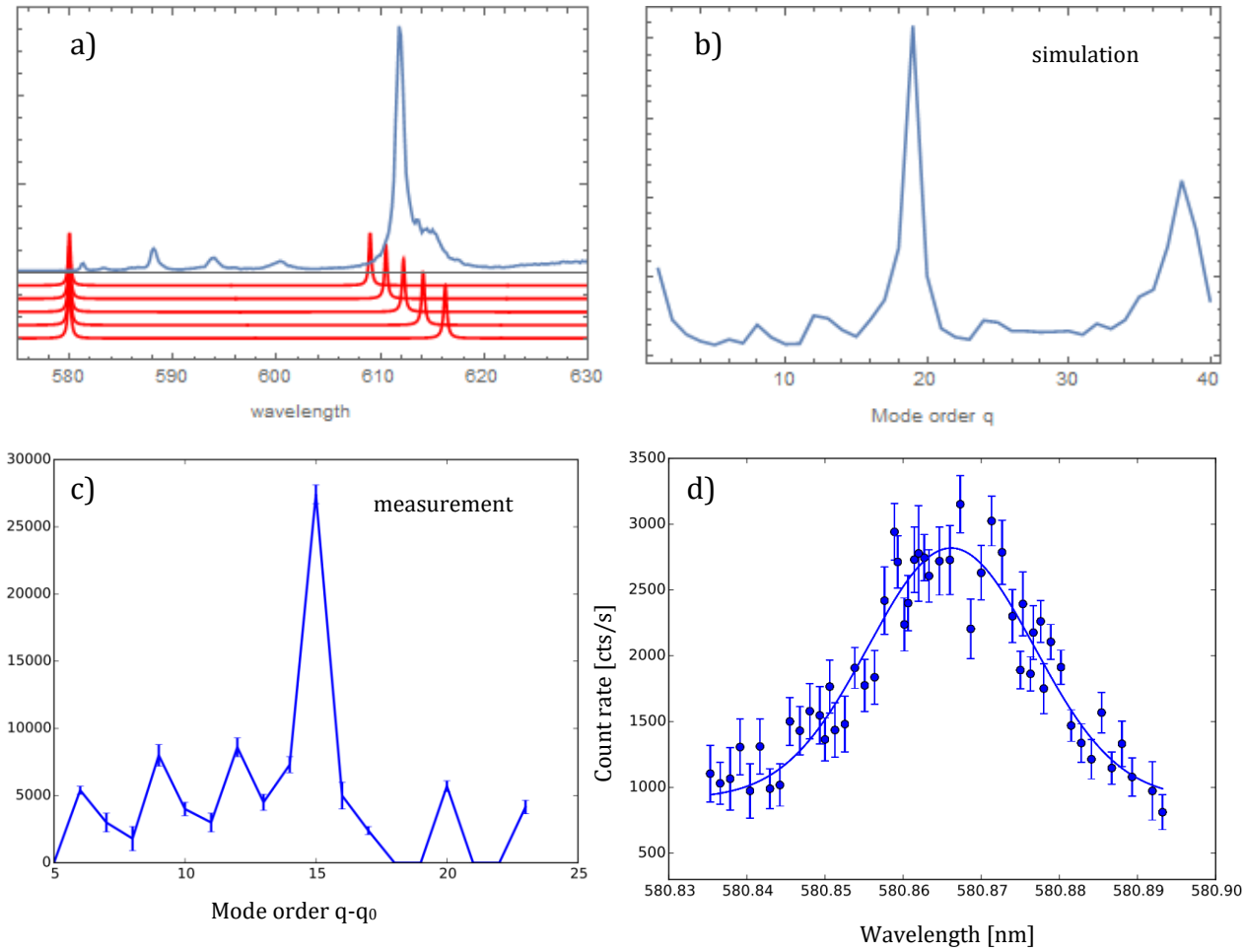

Fig. 5: a) Double resonance scheme showing the free-space spectrum (blue) and cavity transmission spectra for different cavity lengths. b) simulated and c) measured fluorescence count rate as a function of the longitudinal mode order q. Except for an unknown offset q_0, measurement and data show a good agreement. d) Spectroscopy of the inhomogeneous line of the crystal characterized in Fig. 4b).

Measurement scheme

Since stable locking was not possible in the attocube setup due to intrinsic instability and the restrictions of the detection scheme, the measurements were performed in a scanning scheme. Therefore, we modulate the cavity length such that the cavity resonance periodically crosses the transition of the ions. With time-resolved single photon counting on an APD, we infer the average count rate on resonance.

Resonant spectroscopy

We perform spectroscopy by using the above measurement scheme and tune the laser wavelength across the wavelength range of the inhomogeneous line of the $^5D_0$ - $^7F_0$

transition. Figure 5 d) shows the obtained spectrum. We fit with a Gaussian profile and find a FWHM linewidth of 22 GHz, which is comparable to the linewidth in bulk samples and thereby confirms the high crystal quality. We note that this represents the first low-temperature spectroscopy of a single Eu-doped nanocrystal.

Power broadening, estimation of probed ion number and Purcell factor

To understand the origin of the observed spectrum, we consider the average number of ions per homogeneous linewidth. With $N=10^4$ ions in the crystal with an expected homogeneous linewidth of about $\gamma_h = 200$ kHz (J. G. Bartholomew) spread over an inhomogeneous linewidth of $\gamma_{inh} = 22$ GHz, this estimate leads to $n = N\frac{\gamma_h}{\gamma_{inh}} = 0.1$, i.e. the ion transitions are spaced by about 10 linewidths, and low power spectroscopy would in most cases address at most a single ion. To obtain the observed signal, we use a very high excitation intensity (several GW/cm^2), which leads to strong power broadening, and thus off resonant excitation of small ion ensembles.

To calibrate the amount of power broadening, we modulate the frequency of the excitation laser and measure the count rate as a function of the modulation amplitude, see Fig. 6a). We observe a linear signal increase up to an amplitude that corresponds to the cavity linewidth. From an extrapolation of the linear dependence to zero count rate, we can estimate the power broadening. For the measurement shown, it amounts to 140 MHz, which was taken at an intracavity power of ~53mW and an intensity of ~3.5GW/cm^2.

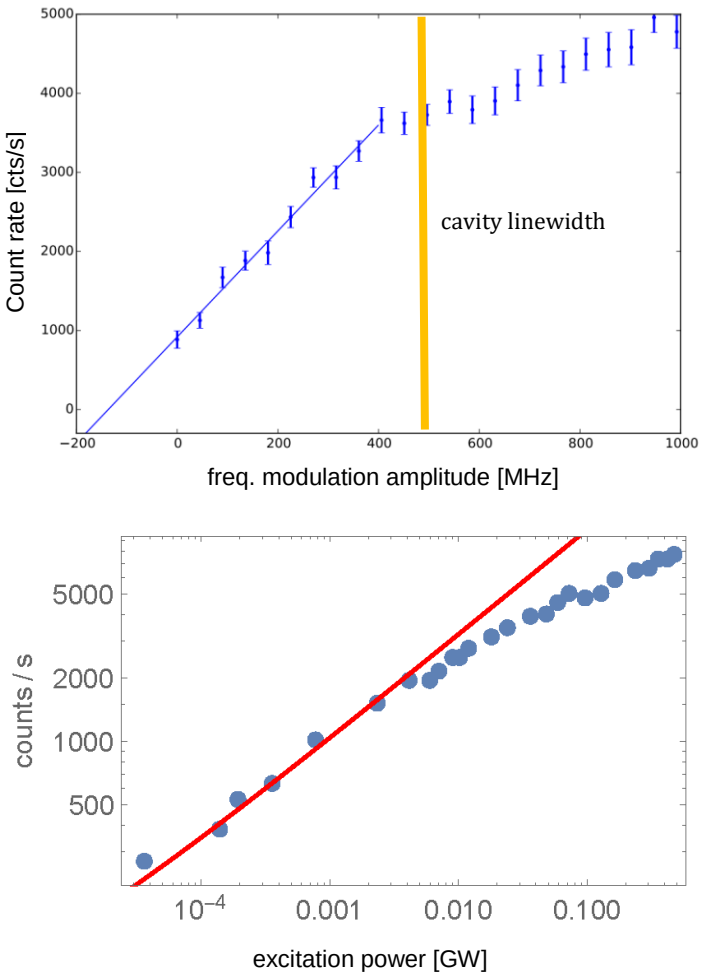

Fig. 6: a) Measured count rate as a function of the laser frequency modulation amplitude for calibration of the power broadening. b) Measured power dependence of the count rate (datapoints) with a fit ~ $\sqrt{power}$ (red line).

We can furthermore measure the count rate on resonance (without modulation) as a function of the excitation power. The scattering rate of a two-level system is given by $R_{sc} = \frac{\gamma}{2}\frac{S_0}{1+S_0+\left(\frac{2\Delta}{\gamma}\right)^2}$, and the power broadened linewidth scales with $\sqrt{S_0} = \frac{\sqrt{2}\Omega}{\gamma}$, where S_0 is the saturation parameter, Ω the Rabi frequency, and γ the excited state lifetime. The observed power dependence shown in Fig. 6b) follows the expected $\sqrt{power}$ dependence over a large range. We can thus rescale the power broadening which we calibrated at high power to the datapoint taken for the lowest excitation power, which is a factor ~400

smaller, such that the broadening is a factor 20 smaller, i.e. ~7 MHz. With an average spectral ion separation of ~1 MHz, this corresponds to probing ~10^1 ions. At this power level, we measure 300 counts/s on resonance, such that the single ion count rate is approximately 30 counts/s, a factor 30 larger than in the confocal measurements discussed above. We can estimate the effective Purcell factor C from the brightness ratio by accounting for the collection and detection efficiency η_{fs} in the confocal case, and the outcoupling and detection efficiency η_c in the cavity case (J. Benedikter): $C = \frac{\eta_{fs}}{\eta_c}\frac{I_c}{I_{fs}}$. With η_{fs} and η_c being similar (~30%), the effective Purcell factor is $C \approx 30$.
While this analysis contains several uncertainties and thus should be regarded as an order of magnitude estimate, it still provides a first indication of the presence of significant Purcell enhancement. We note that we were not able to observe lifetime changes in measurements with pulsed excitation due to the short duration as well as the low overall fraction of time the cavity is on resonance.

Conclusion

We have performed cavity-enhanced spectroscopy measurements of ensembles of Eu ions in an isolated nanocrystal with characterized crystal size, such that an estimation of important parameters such as the number of ions probed and the single ion count rate was possible. As an order of magnitude estimate, we obtain an increase of the single ion photon count rate and a corresponding effective Purcell factor of 30.
Several improvements of the experiments are obvious, most importantly cavity stabilization, but e.g. also the double resonance condition used in the measurements was not ideally fulfilled, and simultaneously enhancing two transitions leads to a leaky channel which is not detected. Selectively enhancing the $^5D_0$- $^7F_0$ transition as required for a stabilized cavity is thus expected to yield higher Purcell factors and signal rates.

References

H. Schniepp, V. Sandoghdar. "Spontaneous Emission of Europium Ions embedded in dielectric nanospheres." *Physical Review Letters* 89 (2002): 257403.

J. Benedikter, H. Kaupp, T. Hümmer, Y. Liang, A. Bommer, C. Becher, A. Krueger, J. M. Smith, T. W. Hänsch, D. Hunger. "Cavity-enhanced single-photon source based on the silicon-vacancy center in diamond." *Physical Review Applied* 7 (2017): 024031.

J. G. Bartholomew, K. de Oliveira Lima, A. Ferrier, P. Goldner. "Optical linew width broadening mechanism at the 10 kHz level for Eu3+:Y2O3 nanoparticles." *NanoLetters* 17 (2017).

M. Mader, J. Reichel, T. W. Hänsch, D. Hunger. "A scanning cavity microscope." *Nature Communications* 6 (2015): 7249.